BUTTERWORTH HEINEMANN

Polymer Vol. 36 No. 26, pp. 5035–5043, 1995

0032-3861/95/$10.00 + 0.00

In situ synthesis of ferrites in ionic and neutral cellulose gels

Louise Raymond, J.-F. Revol and R. H. Marchessault*
Pulp and Paper Research Centre and Chemistry Department, McGill University, 3420 University Street, Montreal, Quebec, Canada H3A 2A7

and D. H. Ryan
Physics Department, McGill University, 3600 University Street, Montreal, Quebec, Canada H3A 2T8
(Received 27 March 1995)

The filaments of a tyrecord rayon were modified by two methods to enhance the degree of swelling of the material: (1) carboxyl and sulfonic acid substituents were introduced into the rayon and (2) the filaments were swollen in sodium hydroxide. The water-swollen filaments were rendered magnetic by *in situ* synthesis of ferrites and the resulting magnetic filaments were characterized by transmission electron microscopy (TEM) and vibrating sample magnetometry (VSM). Two other non-ionic, highly swollen cellulose gels were used as matrices for *in situ* synthesis of ferrites: a never-dried, wet-spun model cellulose filament and a never-dried bacterial cellulose membrane. TEM micrographs of thin cross-sections of the magnetic gels showed that the nanometre-sized ferrites were uniformly distributed whereas the treated rayon filaments had ferrites predominantly at the filament surface. All the materials were superparamagnetic as determined by VSM. However, a ferrimagnetic component was detected after several reaction cycles for the bacterial cellulose membrane by Mössbauer spectroscopy.

(Keywords: superparamagnetic; ferrites; rayon and bacterial cellulose)

INTRODUCTION

Magnetic cellulosics have been prepared by two methods: lumen-loading technology[1–3] and *in situ* synthesis[3–5]. During lumen-loading, magnetic pigments enter the lumen of softwood fibres via the bordered pits, producing a ferrimagnetic fibre which is typically loaded to 15% by weight with pigment. Unbleached Kraft pulp (UBK) and chemithermomechanical pulp (CTMP) from Black Spruce have been loaded with magnetic pigments by this method. Due to the magnetic memory (ferrimagnetism) exhibited by lumen-loaded fibres, applications in information storage, security paper, papermaking and paper handling are being considered.

Synthesizing ferrites via an *in situ* approach within a cellulosic material, such as a super-swollen sodium carboxymethylcellulose (CMC) lap pulp[4], yields nanometre-sized ferrites due to the reaction space constraints of the matrix. Materials prepared by *in situ* synthesis are superparamagnetic: they are easily magnetized in a magnetic field but do not retain magnetization once removed from the field (i.e. they do not have remanence or coercivity). These nanocomposite cellulosic materials show much less colouration than the ferrimagnetic lumen-loaded wood fibres. For this reason, small magnetic particles, of the order of 250 Å are desirable for magnetic coloured toners[6,7]. The lack of magnetic memory of superparamagnetic cellulosics is valuable for biotechnological applications (e.g. antibody separations based on immunoselective absorption using magnetic beads). The desirability of extending *in situ* ferrite synthesis technology to the field of textiles has led to experimentation with continuous filaments such as tyrecord rayon[8]. Magnetic filaments should find use in paper or non-woven fabrics with potential for products such as magnetic filters.

Previously, substrates such as sulfonated thermomechanical wood pulp[4,5], which has carboxylic and sulfonic acid functionalities, were employed for *in situ* synthesis due to their inherent ion-exchange properties. The material absorbed ferrous ions from an aqueous ferrous chloride solution, followed by precipitation of ferrous hydroxide using a mild alkaline treatment. An oxidation step, whereby oxygen gas was bubbled through the suspension, led to the precipitation of nanometre-sized ferrites in the cell wall and at the surfaces of the fibre. After five cycles of the *in situ* reaction, ferrites $\sim$ 20 Å in size were uniformly dispersed across the cell wall. Aggregation of these tiny ferrites was inhibited by the three-dimensional crosslinked network of the highly lignified cell wall. A high concentration of larger ferrites ($\sim$ 100 Å) was present at the fibre surfaces. Since the sulfonic acid content was about the same across the fibre, whereas the iron content was one to two orders of magnitude larger at the fibre surfaces, it was

* To whom correspondence should be addressed

concluded that accessibility and lack of internal reaction space were the major factors influencing ferrite distribution and size. Ongoing studies suggested that neutral cellulose gels would be just as effective as ionic cellulosics and would promote uniform precipitation of ferrites.

This present study was designed to investigate the role of the acid functional groups in preparing magnetic cellulosics via the *in situ* method. In other words, the ion-exchange step as the enabling mechanism for the *in situ* method[7] is questioned. Accordingly, we have used four types of swollen cellulose gels with the goal of synthesizing magnetic iron oxides in the microvoids of these materials. A tyrecord rayon was modified by two methods to create an acidic and a neutral substrate for *in situ* synthesis: in the first method, the filaments were heterogeneously etherified to produce sulfonic and carboxylic acid groups in the rayon and in the second method, the filaments were swollen in sodium hydroxide solutions of various concentrations. The resulting materials were loaded with ferrites by the *in situ* approach and the properties of these two types of modified rayon filament were compared. Two other neutral cellulose gels were used as substrates for *in situ* synthesis: a never-dried, wet-spun model cellulose filament and a never-dried bacterial cellulose membrane. Four major techniques were used to characterize the resulting superparamagnetic materials: optical microscopy, transmission electron microscopy (TEM), vibrating sample magnetometry (VSM) and Mössbauer spectroscopy.

EXPERIMENTAL

Materials

Chemically modified tyrecord rayon. Multifilament yarn from a cone of commercial tyrecord rayon (Courtaulds Canada Inc., Cornwall, Ontario, Canada) was treated with isopropyl alcohol to remove the finish. After washing several times in deionized water, the yarn was air-dried. The rayon filament was heterogeneously etherified with sodium 2-chloroethanesulfonate (CES) and 2,2-dichloroacetic acid (DCA) to introduce sulfonic[9] and carboxylic acid[10] groups into the rayon, respectively.

(a) Etherification using sodium 2-chloroethanesulfonate (CES). Approximately 1 g of cut filaments (~ 2 cm lengths) was etherified by stirring in 15 g of aqueous alkaline solution, prepared from 1 g of CES, 4 g of NaOH pellets and 10 g of deionized water, under a nitrogen atmosphere for 2 min. The reaction vessel was then heated in a water bath at 85 ± 5 °C for specified time intervals (*Table 1*). Following the reaction, the filaments were immediately washed to neutrality with deionized water. A dry etherification method was also attempted, but proved unsuccessful (i.e. a very low acid group content was obtained). The physical properties of the filaments varied with ionic group content: the filaments became brittle with increasing sulfonate content.

$$\text{Cell}^{*}\text{–OH} + \text{ClCH}_2\text{CH}_2\text{SO}_3\text{Na} + \text{NaOH} \rightarrow \text{Cell–O–CH}_2\text{CH}_2\text{SO}_3\text{Na} + \text{NaCl} + \text{H}_2\text{O}$$

(b) Etherification using 2,2-dichloroacetic acid (DCA). The same procedure as in (a) was used, but with DCA reagent. The etherified filaments (*Table 2*) were less brittle than the sulfonated samples. The latter equation implies crosslinking which seemed to be a possible interpretation (described in the discussion section).

$$\text{Cl}_2\text{CHCOOH} + \text{NaOH} \rightarrow \text{Cl}_2\text{CHCOONa} + \text{H}_2\text{O}$$
$$\rightarrow 2\text{Cell–OH} + \text{Cl}_2\text{CHCOONa} + 2\text{NaOH}$$
$$\rightarrow (\text{Cell–O})_2\text{–CHCOONa} + 2\text{NaCl} + 2\text{H}_2\text{O}$$

Swelling the rayon in sodium hydroxide solutions. The rayon was swollen by stirring overnight in sodium hydroxide solutions[11] at various concentrations. Approximately 1 g of filament was cut into 2 cm lengths and was stirred overnight at room temperature in 300 ml of NaOH solutions at various concentrations (see *Figure 3*). The swollen filaments were washed to neutrality with deionized water. The materials swollen with NaOH concentrations less than 3 M in strength had similar mechanical properties to the original rayon.

Model cellulose filaments. Never-dried model filaments of cellulose were obtained by injecting a 12.5% solution of dissolving pulp in *N*-methylmorpholine-*N*-oxide[12] into an excess of distilled water, followed by extensive washing with water. The never-dried filaments contained about 20% cellulose by weight and had a diameter of 1.46 ± 0.01 mm (wet).

Bacterial cellulose membranes. Bacterial cellulose membranes from *Acetobacter xylinum* were kindly

Table 1 Sulfonic acid group contents of tyrecord rayon etherified with 2-chloroethanesulfonate (CES)

Sample	Reaction time (min)	Sulfonate content[a] (eq kg^{-1} ± 0.030)
CES-10	5	0.066
CES-7	6	0.064
CES-9	10	0.148
CES-14	15	0.197
CES-11	20	0.226
CES-13	25	0.447

[a] The sulfonic acid group content of the filaments was determined using conductometric titration (see Experimental)

Table 2 Carboxylic acid group contents of tyrecord rayon etherified with 2,2-dichloroacetic acid (DCA)

Sample	Reaction time (min)	Carboxylate content[a] (eq kg^{-1} ± 0.030)
DCA-1	5	0.087
DCA-2	10	0.144
DCA-3	15	0.185
DCA-4	20	0.234
DCA-6	30	0.254
DCA-8	40	0.277
DCA-10	50	0.291

[a] The carboxylic acid content of the filaments was determined using conductometric titration (see Experimental)

* The abbreviation 'Cell' stands for the anhydroglucose unit of cellulose

provided by K. Watanabe of Bio-Polymer Research Co., Ltd, Kawasaki, Japan. The pellicles produced at the surface of the culture medium were washed and then boiled for 2 h in 4% (w/w) aqueous NaOH to destroy protein. After extensive rinsing in deionized water until neutral, these never-dried membranes were dipped into a 50% ethanol/water solution to preserve them during storage. Prior to experimentation, the membranes were washed thoroughly in deionized water. The membranes contained < 1% cellulose by weight.

X-ray diffraction

A Philips PW 1730 X-ray generator, with a Ni filter to provide Cu $K\alpha$ radiation ($\lambda = 0.1542$ nm), was used to characterize all samples and to study their crystallinities. A flat film cassette was used to record the diffraction patterns in a Warhus camera operated at a film-to-sample distance of 5 cm.

Functional group quantification

Conductometric titration was used to quantify the number of acid functional groups[13,14] in the etherified rayon samples. The cut rayon filaments (~ 2 cm lengths) were acidified by stirring three times in 300 ml of 0.1 M HCI for 1 h. The excess acid was removed by thorough washings with deionized water. The filaments were dispersed in a 0.001 M NaCl solution for the purpose of creating a Donnan equilibrium[15]. The titrations were performed using a previously published methodology[3]. The carboxylated samples showed the characteristics 'plateau' region indicative of weak acid dissociation. The endpoints were determined from the sharp changes in slope and the number of equivalents of acid group was calculated.

Water retention values

The degree of swelling of the etherified and NaOH-swollen rayon filaments was determined using water retention. Approximately 3 g (dry weight) of wet rayon filaments were used for triplicate water retention value determination. Each sample was subdivided into three and placed in uncapped centrifuge tubes. The samples were centrifuged at 900*g* for 30 min. The pads were then transferred to pre-weighed weighing bottles, weighed and dried at 105°C until constant weight. The water retention value (*WRV*) was calculated by dividing the weight of water contained in the sample, following centrifugation, by the dry sample weight.

In situ *synthesis of ferrites*

Ferrites were synthesized in all the materials via a three-step process[4,5]. The modified rayon and never-dried model filaments of cellulose were used in the form of 2 cm lengths. The wet bacterial cellulose membrane was cut into 4 × 4 cm squares prior to ferrite synthesis. Approximately 1 g (dry weight) of material was stirred in 100 ml of $FeCl_2.4H_2O$ solution (0.01 g ml^{-1}) for 1 h, whereby the cellulosic material turned a yellowish colour with time. Sodium hydroxide (50 ml of 0.1 M solution) was added to precipitate ferrous hydroxide. The greenish-black suspension was kept at 65 ± 5°C in a water bath and 10 ml of 10% hydrogen peroxide was added dropwise over a period of 15 min. The sample was removed from the heat and stirred for 1 h in the solution, followed by washing to neutrality with deionized water. The etherified and NaOH-swollen filaments turned a rusty orange colour after one cycle of the *in situ* reaction. The model cellulose filaments turned a ruby red colour which deepened when the material was cycled several times through the reaction. The bacterial cellulose membrane was a rust colour after one cycle of reaction, but became a deeper brown colour upon cycling. The iron content of the etherified and NaOH-swollen filaments did not increase with cycling of the material through the reaction. Significant increases (see *Table 4*) in iron content were seen for the model cellulose filaments and bacterial cellulose membrane with cycling.

Vibrating sample magnetometry

A vibrating sample magnetometer (Physics Department of McGill University) was used to study the magenetic properties of the filaments and membrane after *in situ* synthesis. The samples of the modified rayon and model cellulose filaments used were in the form of 5 mm lengths and the bacterial cellulose membrane was cut into 5 × 5 mm squares which were folded. Approximately 15 mg of each sample was vibrated within a magnetic field of up to 1.5 T and the response of the material was obtained as a function of magnetic field in the form of a magnetic hysteresis loop[16].

Transmission electron microscopy

Samples of magnetized filaments and membrane were successively solvent exchanged with ethanol and propylene oxide, followed by embedding in a Spurr resin which was cured at 70°C overnight. Ultrathin sectioning of the blocks was performed with a Reichert Ultracut E microtome equipped with a diamond knife. The TEM instrument was a Philips EM400 operated at 120 kV for imaging by diffraction contrast in the bright-field mode and for selected area (SA) diffraction.

Mössbauer spectroscopy

Room temperature Mössbauer spectra were obtained for the bacterial cellulose membranes with a conventional constant-acceleration spectrometer in transmission geometry using a 1 Gbq ^{57}CoRh source. The samples were in the form of 2 × 2 cm dried squares of material after one to five cycles of *in situ* reaction. The spectra were fitted using a standard Mössbauer fitting program.

Since the magnetic model cellulose filaments and modified rayon samples were in the form of filaments, a typical Mössbauer experiment using transmission geometry was not feasible[17], therefore a Mössbauer backscattering detector[18,19] was built to study their properties. The detector was a toroidal proportional detector for backscattered X-rays and gamma rays. The detector body was machined from aluminium and consists of two parts with a counting wire (30 μm diameter gold-plated tungsten) which does not lie at the centre of the toroid, but is shifted by 10% of the diameter of the toroidal cross-section towards the axis of the counter. The anode wire is guided by 12 Delrin® posts. The shielding for the source consists of alternating lead and tungsten discs. An aluminized Delrin® window (~ 0.5 mm thick) was used to permit good transmission of the backscattered radiation. The counting gas was a

mixture of 45% argon, 45% krypton and 10% methane at atmospheric pressure.

Backscattering data were obtained for one sample of magnetic model cellulose filament. The sample was prepared by cycling through five cycles of the *in situ* reaction using ferrous chloride solution made from ^{57}Fe metal which was dissolved, under nitrogen, in aqueous hydrochloric acid. The resulting greenish-blue crystals were washed with anhydrous ether and dissolved in deionized water to make up the salt solution. The spectrum was recorded over a period of 2 days and was fitted with a standard Mössbauer fitting program.

Optical microscopy

A Nikon microphot-FXA optical microscope (Nikon Corporation) was used to study the iron distribution across the *in situ*-treated model cellulose filaments and the bacterial cellulose membranes. Sections (12 μm) were cut with a glass knife from the blocks of embedded samples for TEM and mounted on glass slides.

RESULTS AND DISCUSSION

Etherified rayon filaments

The etherification approach was effective in modifying the filaments for *in situ* synthesis (see *Tables 1* and *2*). The sulfonated and carboxylated filaments absorbed more iron than the untreated tyrecord rayon, resulting from a higher degree of swelling of the chemically modified filaments. X-ray diffraction showed a decrease in orientation of the cellulose crystallites following etherification, as a result of swelling. At a sulfonate level of about 200 meq kg^{-1} (*Table 1*), a drastic decrease in strength of the filaments was observed. This was less apparent for the carboxylated samples (*Table 2*). The degree of swelling of the samples was measured by performing water retention experiments. The (*WRV*s) were 3.50 and 1.26 $\pm$ 0.10 for samples CES-14 and DCA-6 (*Tables 1* and *2*), respectively. The carboxylated samples probably swell less than the sulfonated samples because of mild crosslinking of the material during carboxylation.

The *in situ* synthesis reaction was performed on all etherified samples. Samples CES-14 and DCA-6 produced the highest magnetic saturation values of the etherified samples by vibrating sample magnetometry. The magnetization curves are shown in *Figure 1*, from which saturation values of $\sim 0.42\,JT^{-1}kg^{-1}$ for sample CES-14 and $0.30\,JT^{-1}kg^{-1}$ for sample DCA-6 were extracted. The iron contents of these samples, as determined by ashing (±10%), were 2.4 and 0.40% iron by weight for samples CES-14 and DCA-6, respectively. Although the magnetic response of the sulfonated sample was greater than that of the carboxylated sample, the mechanical strength of the carboxylated sample was superior for the reason discussed in the preceding paragraph. All etherified samples exhibited superparamagnetic behaviour by VSM. Cycling the samples through the *in situ* reaction cycle did not increase the iron contents significantly and resulted in increased brittleness of the filaments.

TEM micrographs of sections of samples CES-14 and DCA-6 showed that the ferrites were most highly concentrated at the surface of the filaments. Sample DCA-6 had needle-like ferrites, identified as maghemite (γ-Fe_2O_3) by electron diffraction (*Table 3*), $\sim$ 500 Å long by 60 Å thick, at the surface. A very low concentration of needles, < 300 Å long by 30 Å thick, was present in a few areas inside the filament. *Figure 2* is a TEM micrograph of a section through sample CES-14. At the filament surface of sample CES-14, needles of γ-Fe_2O_3 of dimensions $\sim$ 600 Å long by 60 Å thick predominate, in addition to a lower concentration of discs, identified as magnetite (Fe_3O_4) by electron diffraction (cf. *Table 5*),

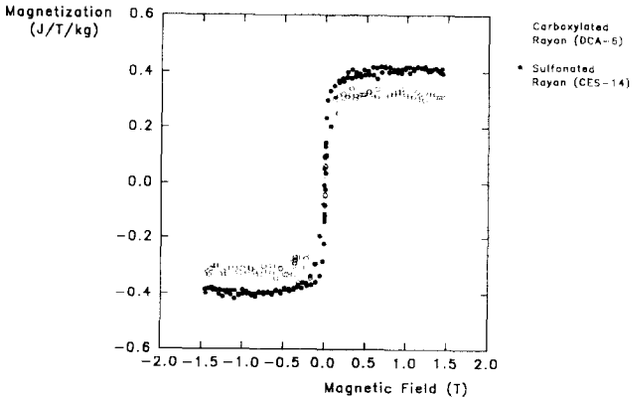

Figure 1 Magnetization curves for samples CES-14 and DCA-6 after one cycle of the *in situ* reaction. The samples have low saturation values and are superparamagnetic

Table 3 Electron diffraction data [*d*-spacing(Å)] for ferrites synthesized *in situ* using rayon filaments swollen in 4 M NaOH after one cycle of reaction. Reference is for maghemite (γ-Fe_2O_3)

In situ ferrites	XRD (reference)[20]
3.25	3.200 56
2.85	2.950 14
2.50	2.514 37
1.90	1.864 43
1.67	1.604 47
1.27	1.272 16

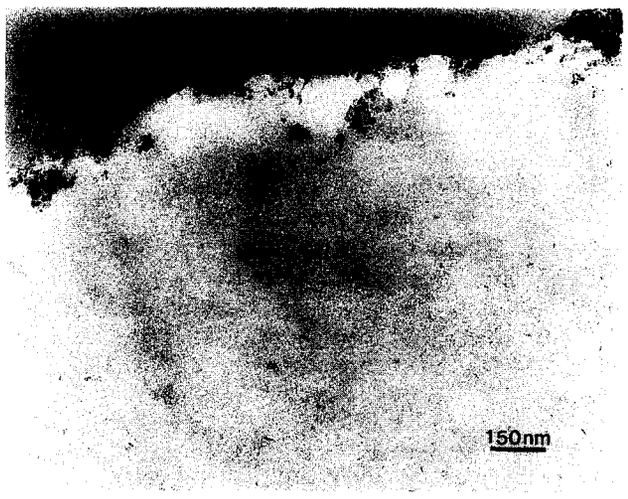

Figure 2 TEM micrograph of a section through sample CES-14 after one cycle of the *in situ* reaction. The surface of the filament is shown at the top of the micrograph. Clusters ($\sim$ 600 Å) of discs of Fe_3O_4 are visible in a large concentration at the surface of the filament and in a lower concentration inside the filament (bottom of the micrograph)

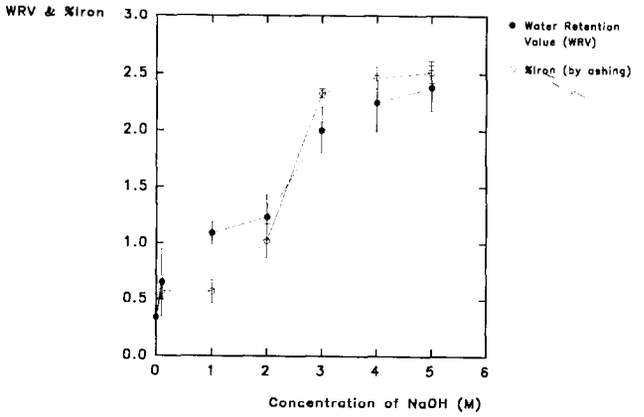

Figure 3 *WRV* and iron content of the NaOH-swollen rayon as a function of the concentration of NaOH. The iron content of the filaments increases as the material swells (increasing *WRV*)

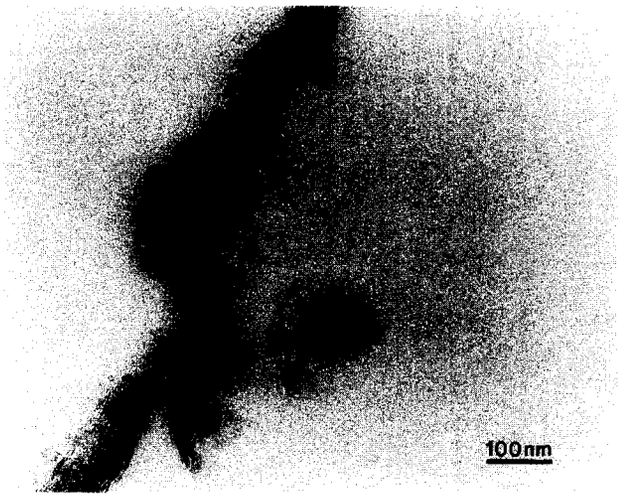

Figure 4 TEM micrograph of a section through a rayon sample swollen in 2 M NaOH after one cycle of the *in situ* reaction. Needle-like ferrites of maghemite, γ-Fe_2O_3, ~ 350–700 Å long by 40 Å thick, are seen at the surface of the filament (towards the left-hand side of the micrograph). No ferrites are visible in the interior of the filament (far right-hand side of the micrograph)

~ 250 Å in size. Clusters (~ 600 Å) of Fe_3O_4 discs are also seen in low concentration at the exterior and in the interior of the filament. Needles of γ-Fe_2O_3 < 300 Å long by 30 Å thick are also dispersed across the interior of sample CES-14. The concentration of ferrites in the interior of sample CES-14 was observed to be larger than for sample DCA-6. The higher degree of swelling of the sulfonated sample promoted accessibility of the filament to iron, resulting in a larger concentration of precipitated ferrites across the interior of the filament and a higher overall iron content.

Filaments swollen in sodium hydroxide

By swelling the rayon filaments in NaOH, *in situ* synthesis could be performed. Without the swelling treatment, the material did not absorb much iron (the first step in *in situ* synthesis). *Figure 3* shows that as the rayon swells (increasing *WRV*), the iron content of the filaments increases in parallel fashion. At a concentration of about 3 M NaOH, the swelling and iron content reach a plateau and the filaments become more brittle. X-ray diffraction showed a loss in orientation of the cellulose crystallites as a result of swelling. The magnetic NaOH-swollen filaments show similar saturation magnetizations to the etherified filaments by VSM. As in the case of the etherified filaments, the iron content of the materials did not increase with cycling of the material through the *in situ* reaction cycle.

TEM of sections of samples swollen in 2 and 4 M NaOH showed a similar ferrite distribution to the etherified samples, whereby a large concentration of needle-like ferrites was seen at the filament surfaces. *Figure 4* is a TEM micrograph of a section of a sample swollen in 2 M NaOH, showing the needles of γ-Fe_2O_3 which range from 350 to 700 Å long and 40 Å thick at the filament surface (left-hand side of the figure). Ferrites were not visible in the interior of the filament (right-hand side of the figure) swollen in 2 M NaOH. Smaller γ-Fe_2O_3 ferrites than those seen at the surface of the filament (~ 180 Å long by 40 Å thick) are distributed in a low concentration throughout the interior of the filament swollen in 4 M NaOH. It seems that as the swelling of the filaments becomes important (*Figure 3*), ferrites grow inside the filament. This was also observed for the etherified filaments, providing supporting evidence that the interior reaction volume is the determining factor in producing a uniform ferrite distribution[5].

Model cellulose filaments

The results obtained with the NaOH-swollen filaments showed that *in situ* synthesis can be performed with a non-ionic substrate. The reaction was then attempted with a more swollen, non-ionic substrate: a never-dried, wet-spun model cellulose filament which contained 80% water by weight. After treating the model cellulose filaments *in situ*, ferrites are loaded within the filament. *Figure 5* is a montage of optical micrographs of sections through four samples of filament: a section through the material as-received (without iron) and after one, three and five cycles of the *in situ* reaction. The iron content of the material increases with cycling (*Table 4*), as seen by the progressive deepening of colour inside the filaments. The iron also seems to be uniformly distributed thoughout the filament, though a slight skin–core structure is visible.

Figure 6 is a TEM micrograph of a section of filament after five cycles of the *in situ* reaction, showing a dense surface dispersion of disc-like ferrites (~ 60 Å) identified as Fe_3O_4 by electron diffraction (*Table 5*). *Figure 7* shows an area near the centre of the filament where clusters of discs of Fe_3O_4 (~ 250 Å) and needle-like γ-Fe_2O_3 ferrites (~ 450 Å long by 60 Å thick) are uniformly distributed. In the centre of the filament (*Figure 8*), clusters of Fe_3O_4 discs ~ 1000 Å in size and needles of γ-Fe_2O_3 ~ 1000 Å long by 100 Å thick are present. TEM of sections of the lower cycle samples (cycles one and three) show similar ferrite distribution and size, but a lower concentration of ferrites is observed.

An air bubble is shown at the left-hand side of *Figure 8*. Bubbles in the filaments were probably formed during processing, producing some of cylindrical shape (those which are continuous through the filament) and others which are not. Of interest is that the ferrites deposit preferentially on the surfaces of these bubbles, as seen by the large concentration of ferrites at the surface of the

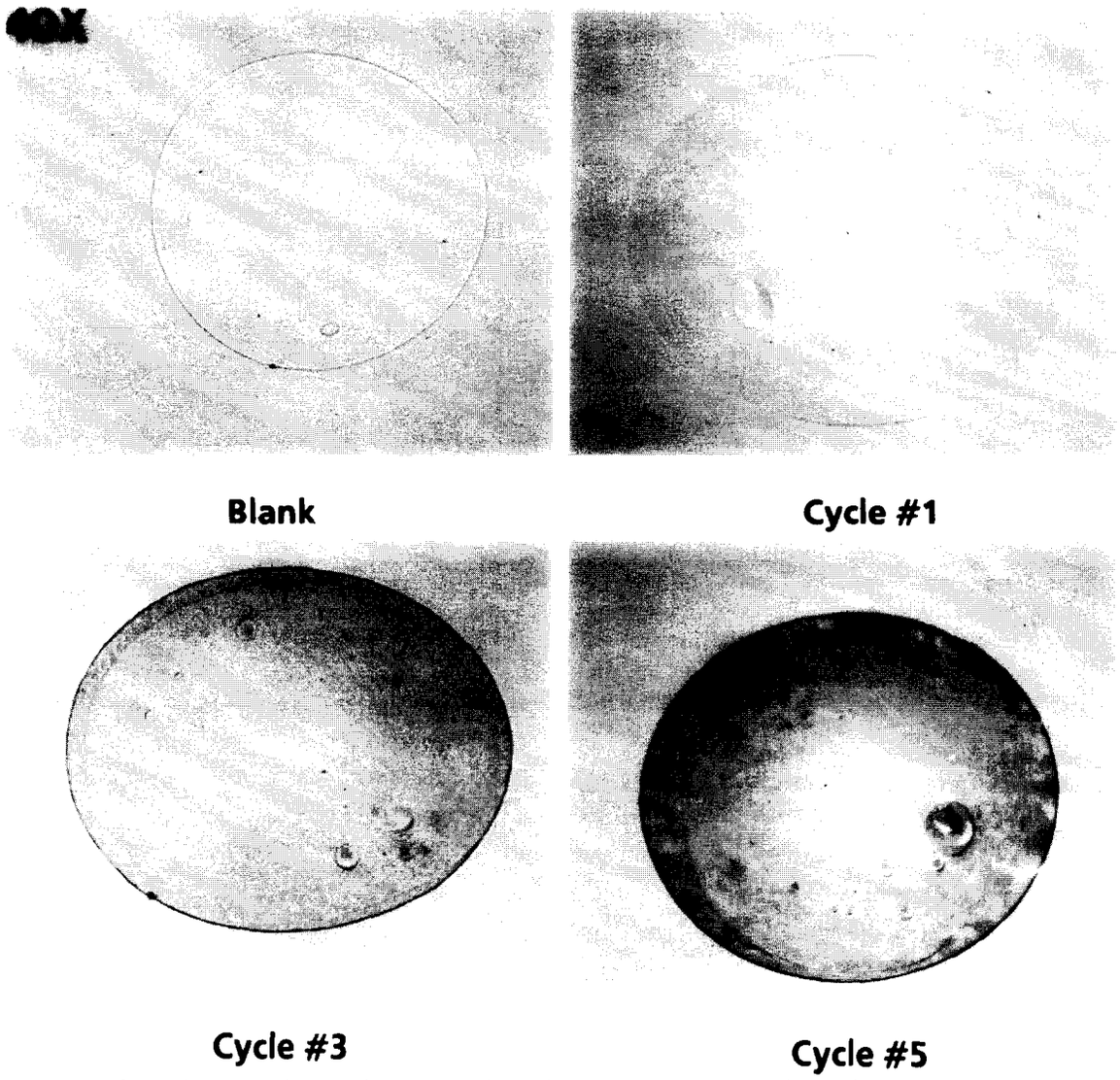

Figure 5 A montage of optical micrographs of sections through the model cellulose filament as-received and after one, three and five cycles of the *in situ* reaction. The iron content of the filaments increases with cycle number

bubble shown in *Figure 8*. This observation provides further proof that accessible reaction space seems to be the major factor in determining ferrite distribution.

The magnetic properties of the filaments were examined using VSM. *Figure 9* shows the magnetization curves for the model cellulose filaments after one to five cycles of the *in situ* reaction. The filaments are superparamagnetic by VSM and the saturation magnetization increases with cycle number up to about $1.2\,J\,T^{-1}\,kg^{-1}$

Table 4 Iron contents[a] for the model cellulose filament and the bacterial cellulose membrane as a function of the number of *in situ* reaction cycles

Cycle no.	Model cellulose filament (%Fe)	Bacterial cellulose (%Fe)
1	0.89	18.69
3	2.13	28.83
5	5.71	37.38

[a] The iron composition (±1%) of the samples was determined by digesting a weighed sample in an acid mixture and analysing spectrometrically using atomic absorption

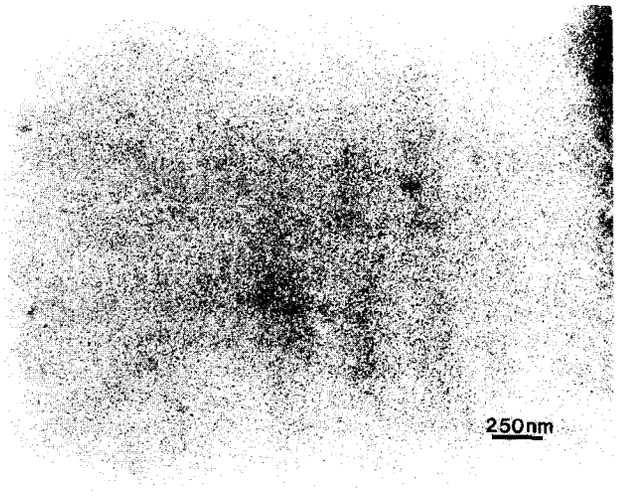

Figure 6 TEM micrograph through a section of a model cellulose filament surface after five cycles in the *in situ* reaction. A dense dispersion of Fe_3O_4 discs (~ 60 Å) is observed

Table 5 Electron diffraction data [*d*-spacing(Å)] for ferrites synthesized *in situ* using model cellulose filament after five cycles of reaction. Reference is for magnetite (Fe_3O_4)

In situ ferrites	XRD (reference)[20]
2.83	2.966 14
2.49	2.532 37
2.31	2.423 53
1.95	2.099 82
1.66	1.615 93
0.99	0.989 60

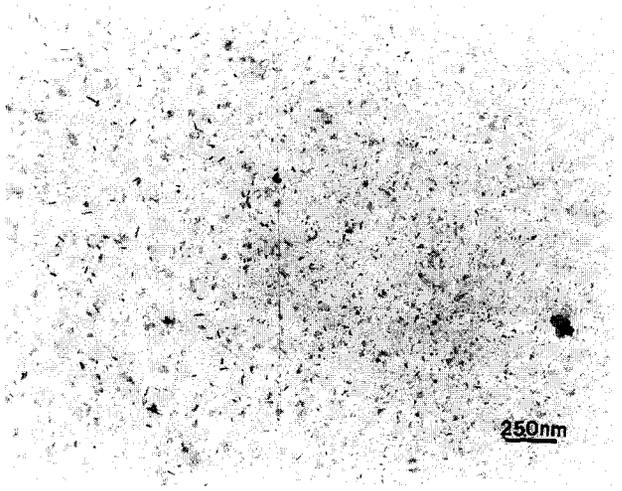

Figure 7 TEM micrograph of a section of the sample described in *Figure 6*, but near the centre of the filament, showing uniformly distributed discs of Fe_3O_4 (~ 250 Å) and needles of γ-Fe_2O_3 (~ 450 Å long by 40 Å thick)

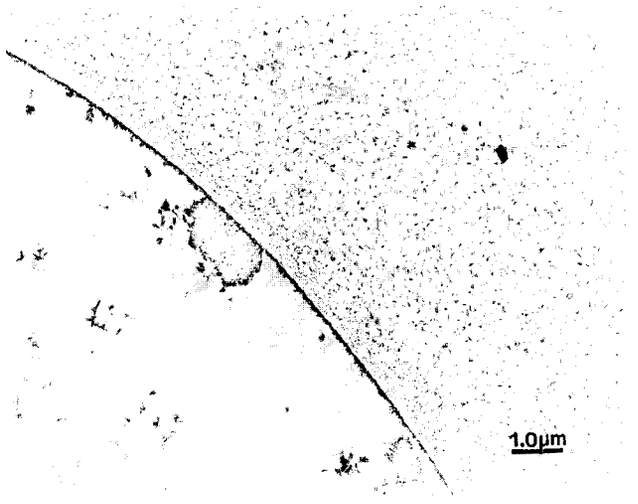

Figure 8 TEM micrograph of the centre of the filament described in *Figure 6*, showing that the size of the ferrites has increased to clusters of discs of Fe_3O_4 (~ 1000 Å) and needle-like ferrites of γ-Fe_2O_3 (~ 1000 Å long by 100 Å thick) in this area. A bubble in the filament is shown at the left-hand side of the figure

for the fifth cycle sample. Information was obtained about the particle-size distribution from the magnetization data for the first, third and fifth cycle samples. The saturation magnetizations for these samples were converted to $JT^{-1}kg^{-1}$ of iron using the iron contents in *Table 4*. Since magnetite in the form of small particles

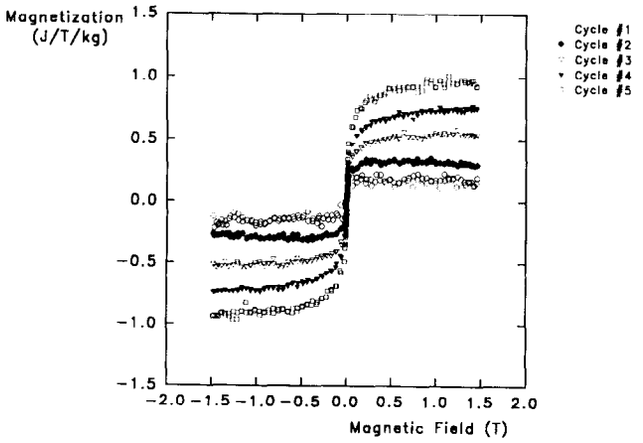

Figure 9 Magnetization curves for the model cellulose filament after one to five cycles of the *in situ* reaction. The saturation magnetization increases with cycling and the filaments are superparamagnetic

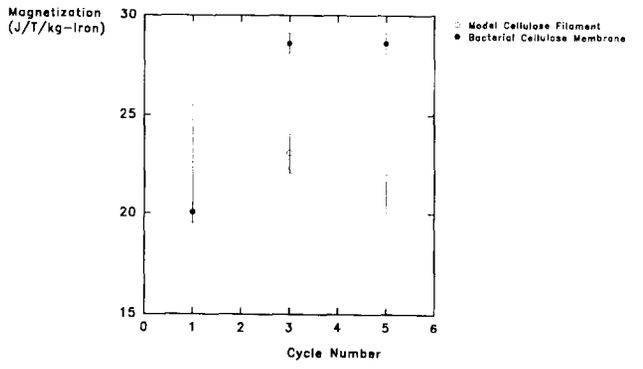

Figure 10 Magnetization in $JT^{-1}kg^{-1}$ of iron as a function of cycle number. Particles do not seem to grow on cycling for the model cellulose filament; however, in the case of the bacterial cellulose membrane, fine particles appear to grow between the first and third cycles of the *in situ* reaction

responds more weakly in a given applied field than larger particles, the same amount of magnetite in fine particle form will give a lower magnetization than that in the form of coarser particles. *Figure 10* shows that the magnetization for the model filaments is small and does not change much with cycle, indicating the presence of fine particles which do not grow on cycling. These results are consistent with the TEM data above. A different trend was observed for the bacterial cellulose membrane, as will be discussed in a following paragraph.

Mössbauer spectroscopy showed that the filaments were superparamagnetic. *Figure 11* is a Mössbauer spectrum of a sample of the model cellulose filament after five cycles of the *in situ* reaction using a backscattering technique (see Experimental). The spectrum consists of a paramagnetic doublet which is characteristic of superparamagnetic materials.

Bacterial cellulose membranes

Since a uniform distribution of ferrites was obtained for the model cellulose filament, precipitation of ferrites in an even more open-textured material was studied. For this purpose, a never-dried bacterial cellulose membrane, which contained about 99% water by weight, was used. Consequently, the iron contents of the membranes after treatment via the *in situ* method were much higher than

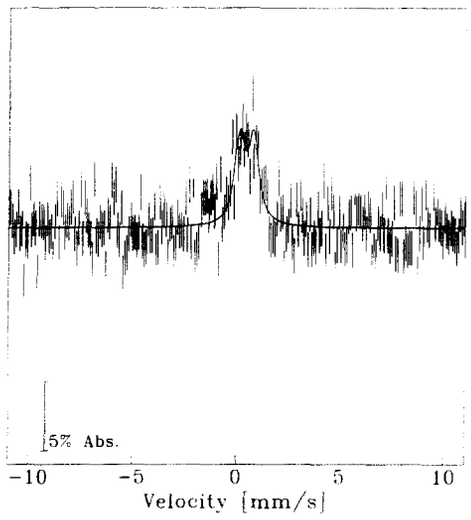

Figure 11 Mössbauer spectrum of the fifth cycle sample of the model cellulose filament sample. The backscattering spectrum shows the presence of a paramagnetic doublet which is characteristic of a superparamagnetic material

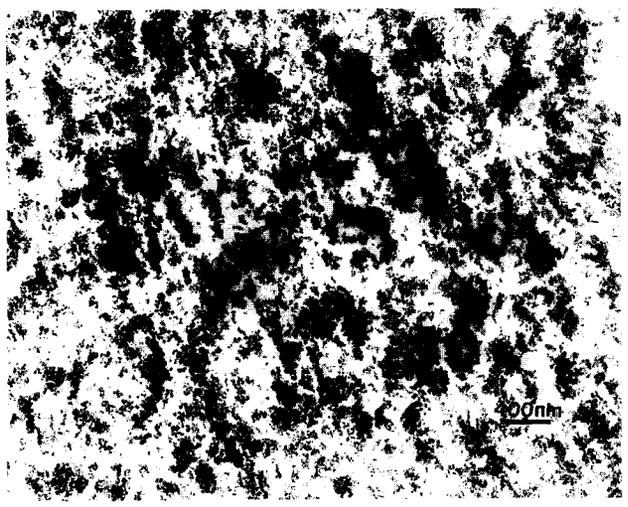

Figure 12 TEM micrograph of a section of the bacterial cellulose membrane after five cycles of the *in situ* reaction. Discs and clusters of $Fe_3O_4 \sim 200$ Å in size, are uniformly dispersed across the membrane

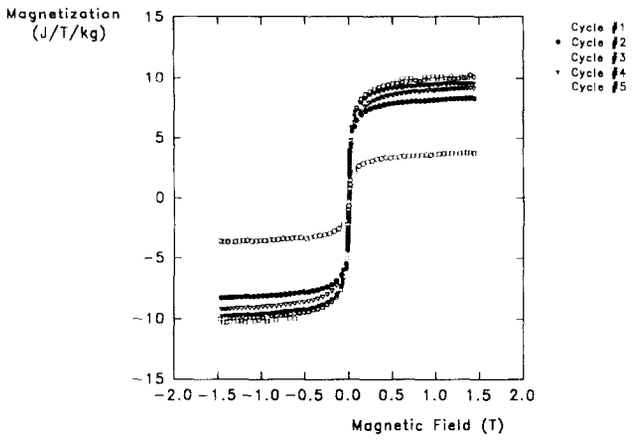

Figure 13 Magnetization curves for the bacterial cellulose membrane after one to five cycles of the *in situ* reaction. Higher saturation magnetizations than in the model cellulose filament have resulted. The samples are superparamagnetic

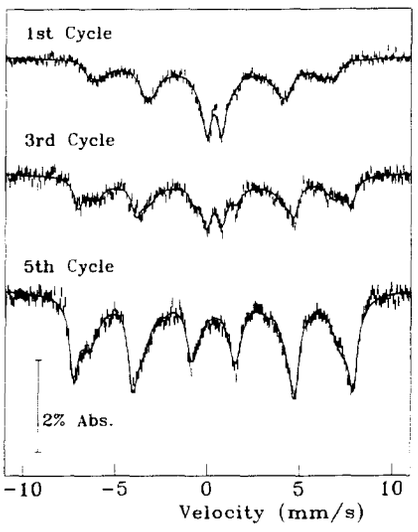

Figure 14 Room temperature Mössbauer spectra of the bacterial cellulose membrane after one, three and five cycles of the *in situ* reaction

in the other materials studied (see *Table 4*) because these membranes had a very large interior reaction space for *in situ* synthesis.

Figure 12 is a TEM micrograph of a section through the membrane treated for five cycles of the *in situ* reaction. Discs and clusters of discs of $Fe_3O_4 \sim 200$Å in size, are dispersed uniformly across the membrane. TEM of sections through the sample treated for one cycle show a lower concentration of ferrite, which is mostly in the form of small particles of γ-Fe_2O_3, in addition to a lower concentration of smaller discs of Fe_3O_4. Larger discs of Fe_3O_4 predominate in the samples treated for more cycles.

The magnetic properties of the membranes after one to five cycles of the reaction were studied using VSM (*Figure 13*). All samples are superparamagnetic by VSM and a jump in saturation value occurs between the first cycle sample and the higher cycle samples. After one cycle, the material saturates at about $3.6\,JT^{-1}kg^{-1}$ and the higher cycle samples have saturations of $\sim 10.5\,JT^{-1}kg^{-1}$. The iron contents for the magnetic bacterial cellulose are shown in *Table 4*. Saturation values for the first, third and fifth cycle samples were converted to $JT^{-1}kg^{-1}$ of iron (as they were for the model cellulose filaments). A jump in saturation value is observed between the first and the higher cycle samples, as seen in *Figure 10*. It seems from these results that the iron deposited as fine particles after the first cycle of reaction grow on cycling. The size of the particles is still in the superparamagnetic regime since bulk magnetite saturates at a value of $124\,JT^{-1}kg^{-1}$ of iron. These results are consistent with the TEM data discussed in the preceding paragraph.

Mössbauer spectroscopy was used to study the magnetic properties of the magnetic bacterial cellulose membranes and for characterization purposes. Due to the time scale of the Mössbauer measurement ($\sim 10^{-7}$ s), static magnetic components not detectable by VSM, which has a time scale of the order of seconds, can be detected. Mössbauer spectra of the first, third and fifth cycle samples of the bacterial cellulose membrane are

shown in *Figure 14*. The first cycle sample shows the characteristic paramagnetic doublet of superparamagnetic materials, indicating that fine particles are present. An additional magnetic component from particles that are large enough to appear blocked at room temperature is also present. The ordered component grows on cycling, providing evidence of particle growth on cycling. This is in agreement with the TEM and VSM results.

CONCLUSIONS

Previously, our work has been concentrated on performing *in situ* synthesis with cellulosic materials having ionic functional groups, such as carboxymethylcellulose and sulfonated thermomechanical wood pulps. In the case of sulfonated wood pulp[5] and a synthetic sulfonated ion-exchange resin (Nafion® 117)[21] it was suggested that accessibility and space were the factors determining ferrite size and distribution. The methodology for creating a uniform ferrite distribution in cellulosics was developed in this present study. The failure of etherified tyrecord rayon filament and NaOH-swollen filament to produce a uniformly iron-loaded material suggested that ionic groups as such are not a requirement for *in situ* synthesis: ionic groups promote swelling and colloidal stabilization rather than any catalytic role in the *in situ* synthesis of ferrites. Thus, it was implied that the more uniform and open voids in a swollen, neutral cellulose gel would perform better for *in situ* synthesis of ferrites.

This hypothesis was pursued and led to experimentation with two swollen cellulosic systems: a never-dried, wet-spun model cellulose filament and a never-dried bacterial cellulose membrane. These materials absorbed larger quantities of iron, compared with the modified rayon described above, and a uniform distribution of ferrites in these materials was observed by optical microscopy and TEM. These materials were superparamagnetic by VSM, as was the case for the modified rayon filament; however, Mössbauer spectroscopy allowed the detection of a ferrimagnetic component for all cycle samples of the magnetic bacterial cellulose membrane. The precipitation of larger ferrites (magnetic component) in the bacterial cellulose membrane was made possible by the much larger voids present in this material. The absence of ionic groups is noteworthy in the context of the previously proposed ion-exchange mechanism of *in situ* ferrite synthesis[5].

Cellulosic nanocomposites can be made using swollen, never-dried, non-ionic cellulosic materials such as wet-spun cellulose filaments and bacterial cellulose membranes. This development offers potential for preparing new nanocomposites from materials not previously considered. For example, the magnetic bacterial cellulose may have properties attractive to the sound industry[22], while the superparamagnetic properties of the cellulose filaments may permit their use in magnetic filtration systems.

ACKNOWLEDGEMENTS

The authors would like to thank Dr Cipei Huang of Shanghai University for preparing most of the etherified rayon samples. We would also like to thank Dr J. -Y. Cavaillé of the Centre de Recherches sur les Macromolécules Végétales (CERMAV), Grenoble, France for the model cellulose filament, and K. Watanabe of Bio-Polymer Research Co., Ltd, Kawasaki, Japan for the bacterial cellulose sample. The assistance of Dr Dorothea Wiarda and S. Kecani of McGill University (Physics Department) in the construction of the backscattering detector for the Mössbauer measurements and Mr Louis Godbout of the Pulp and Paper Research Centre of Canada for help with photography and sectioning is acknowledged. Louise Raymond received a Pulp and Paper Research Centre of Canada (PAPRICAN) student scholarship. This work was supported by Xerox Canada, Inc., Paprican and the Natural Science and Engineering Research Council of Canada.

REFERENCES

1 Ricard, S. and Marchessault, R. H. *MRS Symp. Proc.* 1990, **197**, 319
2 Rioux, P., Ricard, S. and Marchessault, R. H. *J. Pulp Pap. Sci.* 1992, **18**, J39
3 Marchessault, R. H., Rioux, P. and Raymond, L. *Polymer* 1991, **33**, 4025
4 Marchessault, R. H., Ricard, S. and Rioux, P. *Carbohydr. Res.* 1992, **224**, 133
5 Raymond, L. Revol, J. -F., Ryan, D. H. and Marchessault, R. H. *Chem. Mater.* 1994, **6**, 249
6 Andres, R. P., Averback, R. S., Brown, W. L., Brus, L. E., Goddard, W. A., Kaldor, A., Louie, S. G., Moscovits, M., Peercy, P. S., Riley, S. J., Siegel, R. W., Spaepen, F. and Wang, Y. *J. Mater. Res.* 1989, **4**(3), 704
7 Ziolo, R. F., Giannelis, E. P., Weinstein, B. A., O'Horo, M. P., Ganguly, B. N., Mehrotra, V. and Russell, M. W. *Science* 1992, **257**, 219
8 Raymond, L., Huang, C. and Marchessault, R. H. in 'Proc. Hi-Tech Textiles Conf.', Textile World and Association of the Nonwoven Fabrics Industry (INDA), Greenville, USA, 1993, p. 29
9 Timell, C. T. *Svensk Papperstidning* 1948, **11**, 254
10 Hoffpauir, C. L. and Guthrie, J. D. *Textile Res. J.* 1950, 617
11 Warwicker, J. O. in 'Cellulose and Cellulose Derivatives Part 4' (Eds N. M. Bikales and L. Segal), John Wiley & Sons, Inc., New York, 1971, p. 325
12 Maia, E., Peguy, A. and Perez, S. *Acta Cryst.* 1981, **B37**, 1858
13 Scallan, A. M. *Tappi J.* 1981, **66**(11), 73
14 Katz, S., Beatson, R. P. and Scallan, A. M. *Svensk Papperstidning* 1984, **87**, 6
15 Donnan, F. G. and Harris, A. B. *J. Chem. Soc.* 1911, **99**, 1554
16 Jiles, D. 'Introduction to Magnetism and Magnetic Materials', Chapman and Hall, Ltd, London, 1991, p. 52
17 Greenwood, N. N. and Gibb, T. C. 'Mössbauer Spectroscopy', Chapman and Hall, Ltd, London, 1971, p. 251
18 Schaaf, P., Blaes, L., Welsch, J., Jacoby, H., Aubertain, F. and Gonser, U. *Hyperfine Interactions* 1990, **58**, 2541
19 Schaaf, P., Krämer, A., Blaes, L., Wagner, G., Aubertain, F. and Gonser, U. *Nuclear Instr. Meth. Phys. Res.* 1991, **B53**, 184
20 Powder Diffraction File, compiled by JCPDS International Centre for Diffraction Data, USA, 1984
21 Raymond, L., Revol, J. -F., Ryan, D. H. and Marchessault, R. H. 'The precipitation of ferrites in Nafion® membranes' *J. Appl. Polym. Sci.* in press
22 Brown, M. R. in 'Cellulose Structural and Functional Aspects' (Eds J. F. Kennedy, G. O. Phillips and P. A. Williams), Ellis Horwood Limited, West Sussex, 1989, p. 145